Int J Clin Exp Pathol 2018;11(5):2270-2280
www.ijcep.com /ISSN:1936-2625/IJCEP0073243

Original Article

LncRNA UCHL1-AS1 prevents cell mobility of hepatocellular carcinoma: a study based on *in vitro* and bioinformatics

Rui Zhang*, Yichen Wei*, Li'ou Zhu, Lanshan Huang, Yan Wei, Gang Chen, Yiwu Dang, Zhenbo Feng

*Department of Pathology, The First Affiliated Hospital of Guangxi Medical University, Nanning 530021, Guangxi Zhuang Autonomous Region, China. *Equal contributors.*

Received January 22, 2018; Accepted March 8, 2018; Epub May 1, 2018; Published May 15, 2018

Abstract: We set out to investigate biological functions and potential molecular mechanisms of long non-coding RNA (lncRNA) in hepatocellular carcinoma (HCC). HCC cell line Bel-7404 was cultured and transfected with antisense to the ubiquitin carboxyl-terminal hydrolase L1 (UCHL1-AS1). Viability and mobility were detected by MTT and wound healing assays. Additionally, enrichment analysis and functional networks of UCHL1-AS1 related genes in HCC were performed. Results showed that high level UCHL1-AS1 could effectively inhibit HCC cell migration. However, there was no significant correlation between overexpressed UCHL1-AS1 and HCC proliferation. Meanwhile, BMP4, CALM3, and HRAS were selected from 204 genes that related to UCHL1-AS1. All of these hub genes play critical roles in HCC occurrence and development. Thus, underlying molecular mechanisms among hub genes and UCHL1-AS1 in HCC might be valuable for prognosis and treatment.

Keywords: Long non-coding RNAs, UCHL1-AS1, hepatocellular carcinoma, mobility, bioinformatics

Introduction

As the most common liver cancer worldwide, hepatocellular carcinoma (HCC) ranks highly in overall cancer-related deaths [1, 2]. A variety of main factors causing HCC have been reported such as hepatitis B or C infections, alcohol abuse, and aflatoxin B1 [3]. Currently, surgical resection, liver transplantation, and chemotherapy are considered as available treatment strategies for HCC [4]. However, frequent metastasis and recurrence have induced a lower 5-year overall survival of HCC patients [5, 6]. Moreover, high resistance to chemotherapy has led to poor prognosis of HCC [7, 8]. Dysregulation of growth factors and receptors and signaling pathways could influence HCC's development and prognosis [9]. Therefore, it is necessary to investigate potential molecular targeting mechanisms for enhancing treatment efficiency and prognostic conditions of HCCs.

Long non-coding RNAs (lncRNAs) are a novel group of non-coding RNAs > 200 nucleotides, which play pivotal roles in different processes of cell biology and pathology. LncRNAs have been broadly examined in tumors and some new functions of lncRNAs have updated our awareness of their roles in tumor incidence, development, and distinct therapeutic options. Deregulation of some lncRNAs in cancers has potential to act as a favorable marker for cancer surveillance, early diagnosis, and postoperative monitoring.

Some studies have determined that aberrant expression levels of certain lncRNAs have been observed in HCC, one of the most common cancers all over the world. Previously, expression levels of a spliced lncRNA antisense to the ubiquitin carboxyl-terminal hydrolase L1 (UCHL1), namely, UCHL1-AS1, has been detected by our group to be clearly downregulated in HCC tissues. Moreover, we found that downregulation of UCHL1-AS1 was evidently related to progression of HCC, as reflected by its correlation with the status of portal vein tumor thrombus and distant metastasis [10]. However, the biological function of UCHL1-AS1 on HCC cells remains

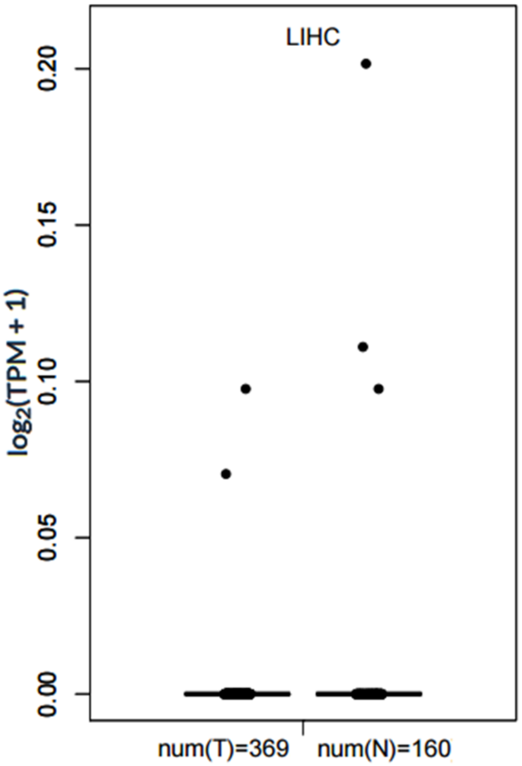

Figure 1. Expression level of UCHL1-AS1 in HCC from Gene Expression Profiling Interactive Analysis (GEPIA). Transcripts Per Million (TPM) was calculated and expression level of a gene was presented by using Log_2 (TPM+1) Scale. Cutoff value was 1 for $|\text{Log}_2\text{FC}|$ and 0.05 for *P*-value. Due to the small sample size, no possible statistical analysis could be conducted.

unknown as well as its prospective molecular mechanism in HCC. Thus, we investigated the effect of UCHL1-AS1 on proliferative ability and mobility of HCC cells.

Materials and methods

Expression levels of UCHL1-AS1 in HCC tissues from TCGA project

Expression levels of UCHL1-AS1 in HCC and non-HCC controls were achieved from Gene Expression Profiling Interactive Analysis (GEPIA), which re-analyzed data from The Cancer Genomic Atlas (TCGA). Transcript Per Million (TPM) was calculated and expression level of a gene was presented by using Log_2 (TPM+1) Scale. Cutoff value was 1 for $|\text{Log}_2\text{FC}|$ and 0.05 for *P*-value. Meanwhile, expression levels of UCHL1-AS1 in 21 HCC cell lines and normal tissues were achieved from Cancer Cell Line Encyclopedia (CCLE) and three BioProjects: Illumina bodyMap2 transcriptome (https://www.ncbi.nlm.nih.gov/bioproject/PRJEB2445/), total RNA sequencing from 20 human tissues [11], and HPA RNA-seq normal tissues [12].

Cell culture and transfection

HCC Bel-7404 cell line was achieved from Shanghai Institute of Cell Biology (Shanghai, China) and incubated in high glucose Dulbecco's Modified Eagle's Medium (DMEM) (Wisent, Nanjing, China) supplemented with 10% fetal bovine serum (Si-Ji-Qing, Hangzhou, China) in an atmosphere with 5% CO_2 at 37°C. Bel-7404 cells were stably transfected with Lentiviral Vector (LV) to establish the cell model of over-expressed UCHL1-AS1. The current study design included three groups: blank control (BC), negative control (NC), and experimental group (LV-UCHL1-AS1). Bel-7404 cells were plated on six-well plates and transfected using 8 μL Lipofectamine 2000 (Invitrogen, CA), following manufacturer instructions. The medium was replaced at 8-12 hours post transfection and culturing proceeded. Finally, cells were collected at 48 hours post-transfection for further research.

RNA isolation and RT-qPCR for UCHL1-AS1

Total RNA was extracted from cultured cells using TRIzol Reagent (Invitrogen, USA). Reverse transcription of isolated RNA was performed using PrimeScript RT reagent kit (Takara, China), according to manufacturer instructions. RT-qPCR was performed by Light Cycler 480 (Roche, Switzerland) with a SYBR Green Master Mix (Roche, Switzerland). The primers were designed by our group and synthesized by Invitrogen as follows: UCHL1-AS1, the forward primer 5'-AGCGTGAGCAAGGAGAA-3', the reverse primer 5'-GGAAGAGGGGAAATCAGCAA-3'; internal controller ß-actin, the forward primer 5'-GCACCACACCTTCTACAATGAGC-3', and the reverse primer 5'-GGATAGCACAGCCTGGTAGCAAC-3'. The steps of PCR were set up as follows: an initial denaturation at 95°C for 15 minutes, denaturation step lasted 10 seconds 95°C, annealing at 60°C for 30 seconds, and extension at 72°C for 30 seconds. Finally, UCHL1-AS1 levels were expressed by the $2^{-\Delta\Delta Cq}$ comparative method [13-17].

Figure 2. Expression level of UCHL1-AS1 in pan-cancer from Gene Expression Profiling Interactive Analysis (GEPIA). Transcripts Per Million (TPM) was calculated and the expression level of a gene was presented by using Log_2 (TPM+1) Scale. Cutoff value was 1 for $|Log_2FC|$ and 0.05 for *P*-value. Different expression patterns of UCHL1-AS1 were observed in distinct cancer types. Each dot represents sample expression.

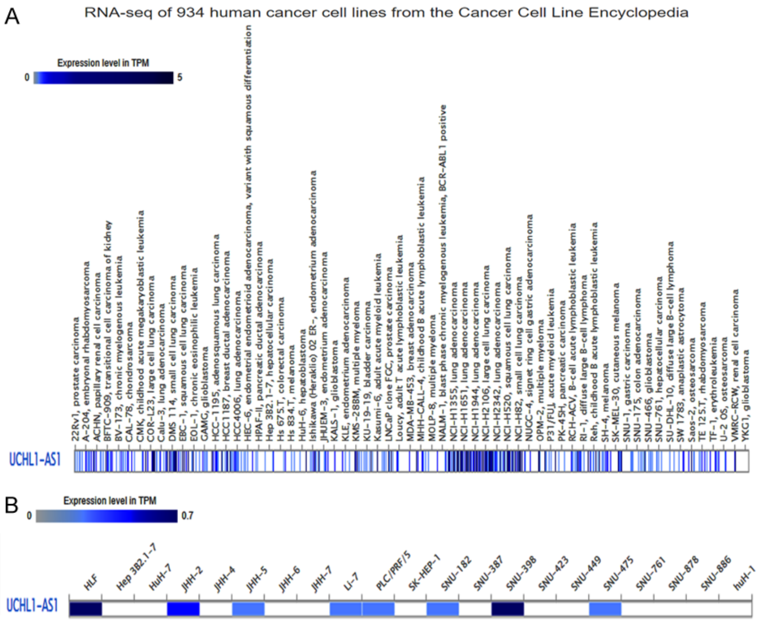

Figure 3. Expression level of UCHL1-AS1 in cell line of pan-cancer from Cancer Cell Line Encyclopedia (CCLE). Transcripts Per Million (TPM) was calculated. Different expression pattern of UCHL1-AS1 could be observed in distinct cancer types. A. Pan-cancer cell lines; B. HCC cell lines.

MTT assay

Viability of HCC cells overexpressing UCHL1-AS1 was detected by MTT assay. HCC cells in logarithmic phase were digested with enzymes and turned into a single cell liquid. We plated 4 × 10^3 cells per well in 96-well plates and cultured in an environment with 5% CO_2 at 37°C. Each well would be added 20 μl MTT (Sigma, USA) at 24 hours, 48 hours, 72 hours and 96 hours, respectively. After 4 hours of incubation of cells, medium was aspirated and 150 μl DMSO (Solarbio, Beijing, China) was added. Subsequent to cells shaking for 10 minutes, values of optical density (OD) for each sample were measured at 570 nm by

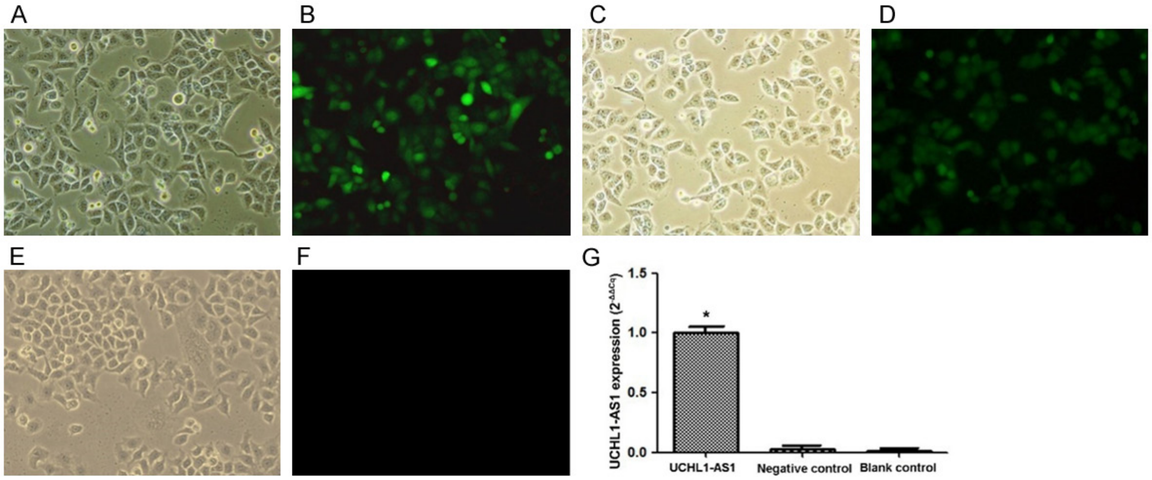

Figure 4. Transfection efficiency and expression levels of UCHL1-AS1. A, B. Transfection efficiency assay of human HCC cell line Bel-7404 48 h post transfection in LV-UCHL1-AS1 group (× 400 times); C, D. Transfection efficiency assay of human HCC cell line Bel-7404 48 h post transfection in negative control group (× 400 times); E, F. Transfection efficiency assay of human HCC cell line Bel-7404 48 h post transfection in blank control group (× 400 times); G. Expression of transfected UCHL1-AS1 in Bel-7404 48 h post transfection. **P* value < 0.05.

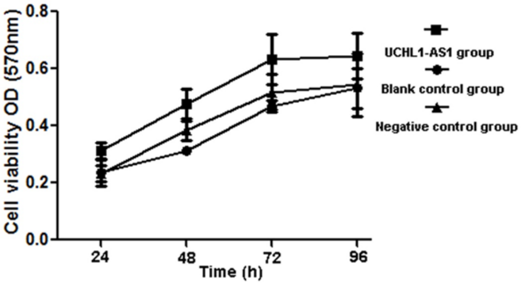

Figure 5. Cell growth rate curves of HCC cells Bel-7404 transfected with UCHL1-AS1 in different groups.

a microplate reader. Three experimental groups were performed in triplicate and cell viability was achieved and calculated.

Scratch testing

Three groups of cells growing in logarithmic phase were cultured in 6-well cell plates. We drew a trace on the surface of cultured cells using a pipette tip when the density of cells reached 90%. After culturing in high glucose DMEM (Wisent, Nanjing, China) without serum for 24 hours, the healing area of scratch was observed and pictured at 0 hours, 24 hours, 48 hours, 72 hours and 96 hours. Image J was used for determination of scratch testing [18]. Scratching width among 3 groups was calculated using Student's t-test and one-way Analysis of variance (ANOVA) by SPSS version 22.0 (Chicago, IL, USA).

Related gene collection and pathways annotation

Genes correlated to UCHL1-AS1 in HCC were collected from Tanric (http://ibl.mdanderson.org/tanric/_design/basic/index.html). The Database for Annotation, Visualization, and Integrated Discovery (DAVID) (https://david.ncifcrf.gov/) was used for Gene Oncology (GO) and Kyoto Encyclopedia of Genes and Genomes (KEGG) investigation. All significant pathways related to UCHL1-AS1 in HCC were presented by ImageGP (http://www.ehbio.com/ImageGP/) and integrated by the plugin of ClueGO from Cytoscape (v 3.5.1), which helped analyze prospective functions of cross-talk genes. Meanwhile, protein-protein interaction (PPI) of these UCHL1-AS1-related genes was outlined by STRING. Expression data of selected hub genes in HCC were downloaded from TCGA database (level 3).

Results

Expression levels of UCHL1-AS1 in HCC tissues from TCGA project

Previously, we reported downregulation of UCHL1-AS1 in HCC tissues detected by real time RT-qPCR with clinical samples from our

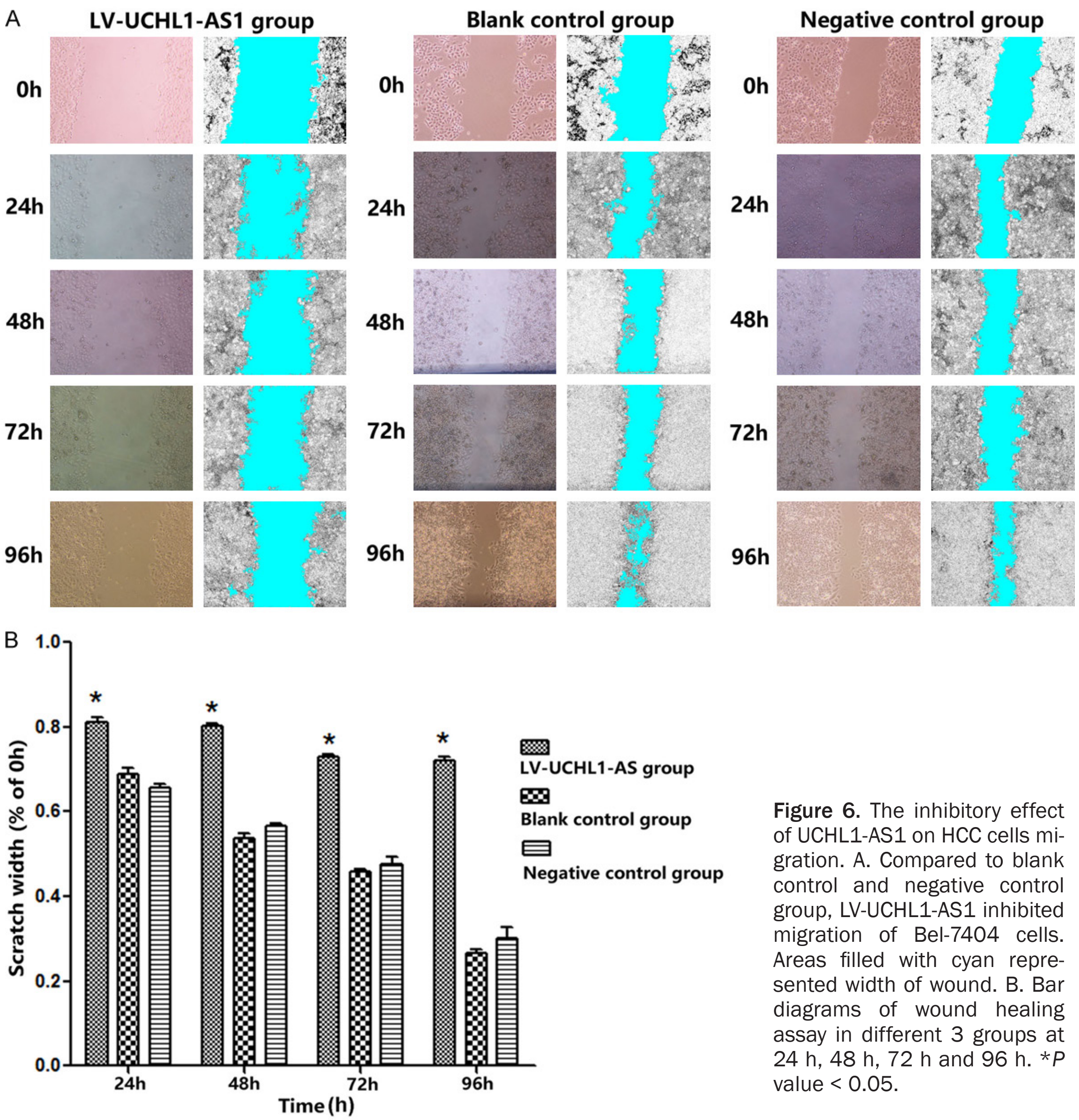

Figure 6. The inhibitory effect of UCHL1-AS1 on HCC cells migration. A. Compared to blank control and negative control group, LV-UCHL1-AS1 inhibited migration of Bel-7404 cells. Areas filled with cyan represented width of wound. B. Bar diagrams of wound healing assay in different 3 groups at 24 h, 48 h, 72 h and 96 h. **P* value < 0.05.

Table 1. Width of wound healing assay in LV-UCHL1-AS1 group, blank control group, and negative control group

Time (h)	Width (% of 0 h)		
	LV-UCHL1-AS1 (Mean ± SD)	Blank controls (Mean ± SD)	Negative controls (Mean ± SD)
0	1.00 ± 3.00	1.00 ± 3.05	1.00 ± 1.73
24	81.07 ± 1.22	68.90 ± 1.39	65.63 ± 0.75
48	80.27 ± 0.46	53.80 ± 1.20	56.53 ± 0.75
72	73.07 ± 0.46	45.80 ± 0.69	47.43 ± 1.99
96	72.00 ± 0.80	26.70 ± 0.69	30.00 ± 2.60
P value	P < 0.01, F = 90.304		

Note: SD, standard deviation.

institution [10]. To further confirm this finding, we attempted to collect relative data from publically available sources including TCGA, GEO, ArrayExpress, and literatures. Unfortunately, only TCGA provided an extremely small sample size with UCHL1-AS1 in HCC tissues (**Figure 1**), therefore, the original plan to perform a comprehensive meta-analysis could not be accomplished. Since RNA-seq data were limited due to sample size, we collected UCHL1-AS1 expression patterns in pan-cancer and found that it was tumor-specific (**Figure 2**). To achieve more information on expression levels of UCHL1-AS1 in HCC, we found that different expression levels could

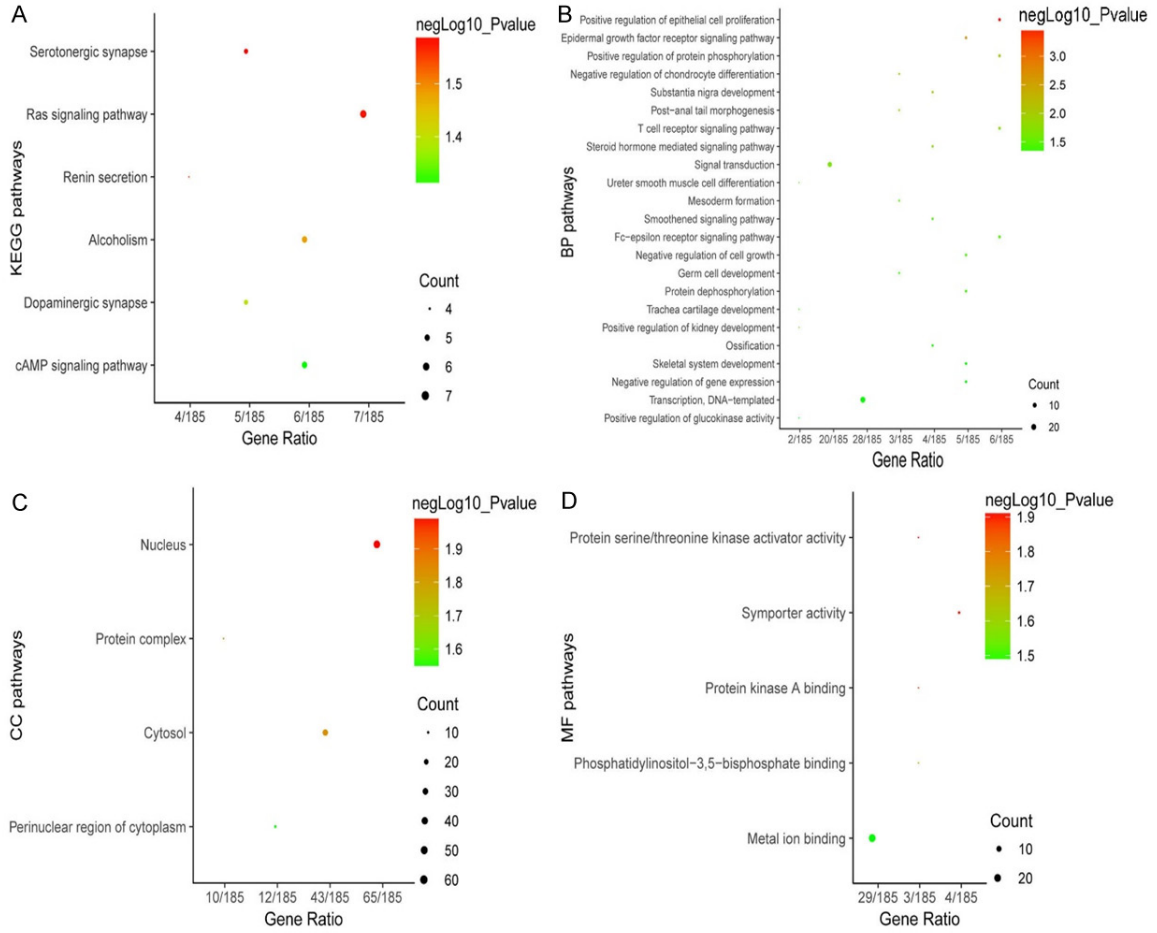

Figure 7. Enrichment scatter plot of UCHL1-AS1 correlated genes in KEGG, BPs, CCs, and MFs. A. Kyoto Encyclopedia of Genes and Genomes (KEGG) pathways scatter plots; B. Biological process (BP) enrichment plots; C. Cellular component (CC) enrichment plots; D. Molecular function (MF) enrichment plots. Red nodes mean a higher efficiency and bigger nodes represent a larger counts of involved genes.

be found in various cell lines including 21 HCC cell lines from CCLE (**Figure 3**). But none of the three BioProjects revealed that UCHL1-AS1 mRNA could be detected in non-HCC liver tissues (data not shown). Thus, the expression status of UCHL1-AS1 in HCC and normal liver tissues still needs to be investigated with a larger sample size in a new independent cohort.

Transfection of UCHL1-AS1 into HCC Bel-7404 cells

Transfection efficiency was monitored via fluorescence observed by microscope (**Figure 4A-F**) and real time RT-qPCR (**Figure 4G**) 48 hours post transfection, which indicated a successful transfection of UCHL1-AS1 into HCC Bel-7404 cells.

Proliferation of overexpressed UCHL1-AS1 HCC cells

We further investigated the influence of UCHL1-AS1 on proliferation of HCC cells by MTT assay. Cell viability was intuitively revealed via cell growth rate curves (**Figure 5**). The results revealed that compared with the blank control and negative control groups, overexpressed UCHL1-AS1 insignificantly inhibited cell proliferation ($P > 0.05$).

Overexpression of UCHL1-AS1 inhibited HCC cell mobility

Scratch wound test was used for investigating effects of overexpressed UCHL1-AS1 on cell migration in HCC cases. The number of migrated cells in wound areas of BC and NC groups increased quickly from 24 hours to 96 hours

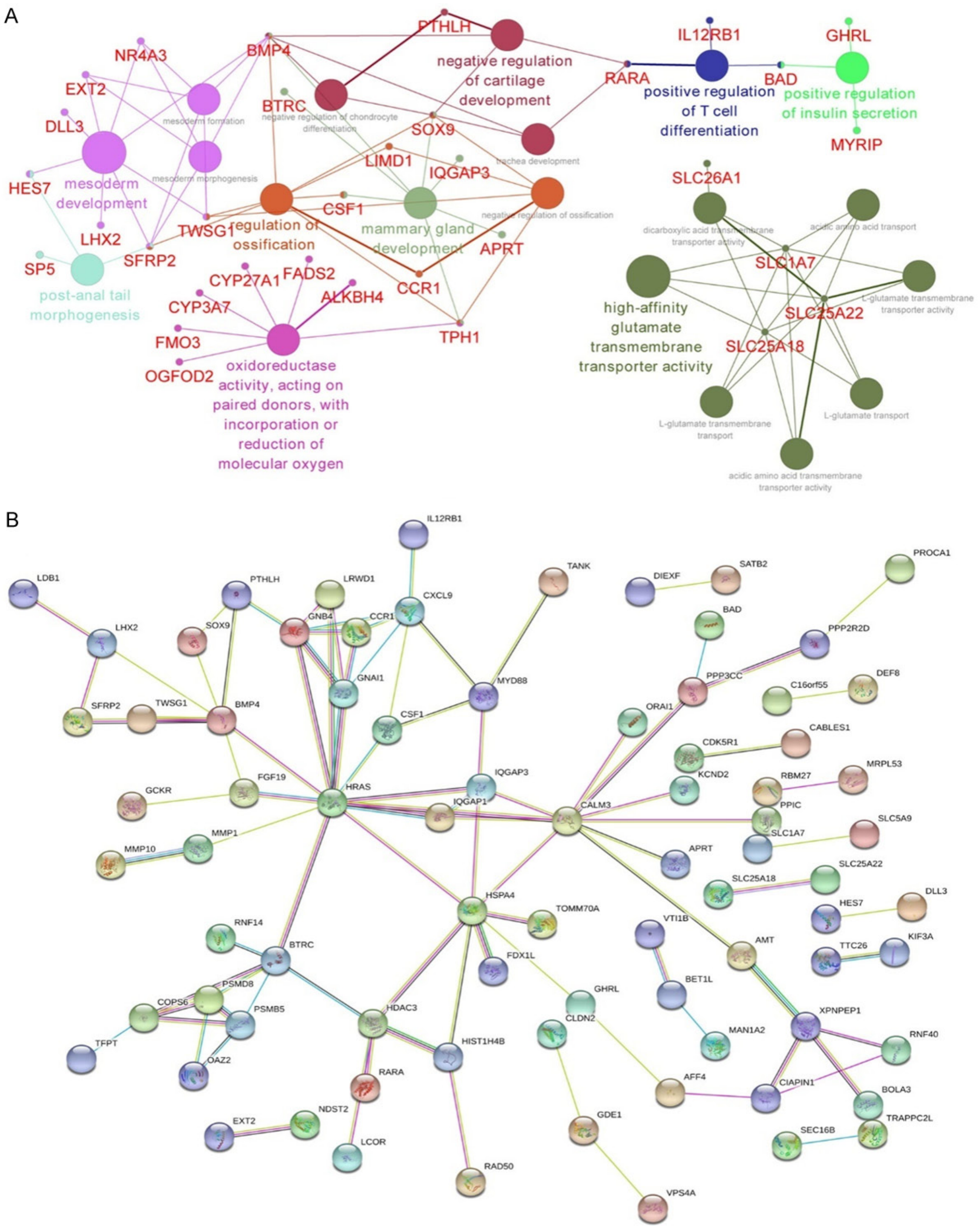

Figure 8. Functional networks of UCHL1-AS1 related genes in HCC. A. Relations network of enriched pathways and genes by ClueGO; B. Protein-Protein Interaction (PPI) network.

(**Figure 6A**, **6B**). Additionally, compared with BC and NC groups separately, the width of UCHL1-AS1 group was significantly wider ($P < 0.01$) (**Table 1**). These evidences manifested that overexpression UCHL1-AS1 could suppress migration of Bel-7404 HCC cells *in vitro*.

Enrichment analysis and potential hub genes of UCHL1-AS1

A total of 204 genes that related to UCHLI-AS1 in HCC were extracted. KEGG pathways and GO enrichment terms were analyzed, respectively

Table 2. The top 10 protein-protein interactions

Node 1	Node 2	Coexpression	Experimentally determined interaction	Database annotated	Automated textmining	Combined score
PSMB5	PSMD8	0.705	0.994	0.9	0.365	0.999
GNAI1	GNB4	0.164	0.827	0.9	0.512	0.992
CXCL9	CCR1	0	0	0.9	0.626	0.961
CALM3	PPP3CC	0.056	0.904	0	0.587	0.959
HRAS	IQGAP1	0.053	0.178	0.9	0.546	0.959
HDAC3	RARA	0	0.367	0.9	0.358	0.955
GNAI1	HRAS	0.105	0.173	0.9	0.456	0.954
HRAS	FGF19	0	0.097	0.9	0.358	0.936
CSF1	HRAS	0	0	0.9	0.357	0.933
IL12RB1	CXCL9	0	0	0.9	0.323	0.929

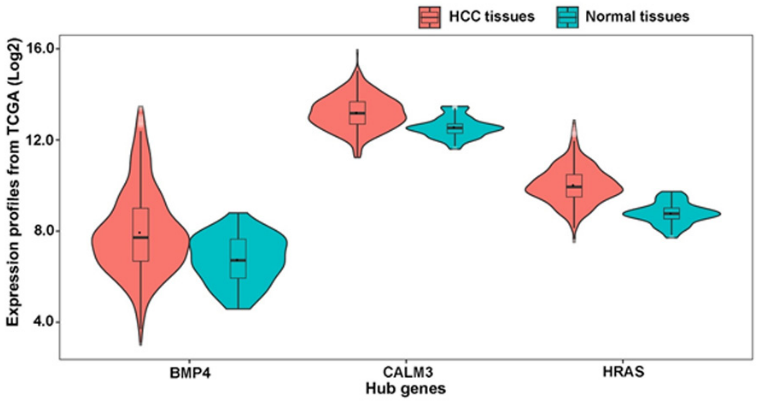

Figure 9. The 3 hub genes levels in HCC from TCGA database.

(**Figure 7A-D**). In KEGG pathways, the most significant one was 'serotonergic synapse' (P = 0.0257). GO was composed by biological process (BP), molecular function (MF), and cellular component (CC). Six genes functioned in 'positive regulation of epithelial cell proliferation' which was the most significant term of BPs (P = 0.0003). In addition, 'nucleus' (P = 0.0102) and 'protein serine/threonine kinase activator activity' (P = 0.0123) were most effective in CCs and MFs. Networks of functionally grouped genes were outlined by ClueGO and PPI (**Figure 8A**, **8B**). The PPI network contained 184 interactions among UCHL1-AS1 related genes. The top 10 interactions are listed in **Table 2**. Meanwhile, genes HRAS, BMP4 and CALM3 which interacted with various genes over 6 times were selected as hub genes. Expression levels of these 3 hub genes in 374 HCC patients were compared with 50 normal cases (**Figure 9**). Interestingly, we found that all 3 hub genes showed significantly higher levels in HCC tissues (P < 0.0001) (**Table 3**).

Discussion

RNA sequences that transcribe from the opposite direction at the same locus of DNA strands leads to natural antisense transcripts. Sense-antisense pairs might be formed from over 20% and is a usual manifestation in the human genome [19, 20]. However, a mass of endogenous RNA antisense transcripts has been found to be in a wide variety of eukaryotic organisms [21, 22]. Previously, studies have demonstrated that natural antisense transcripts carry out a role of regulator in gene levels by affecting mRNA transcription, translation, and processing [20, 23]. Dysfunction of natural antisense transcripts could be closely related with human diseases. Furthermore, as a type of endogenous cellular RNAs with no open reading frame, lncRNAs function both in nuclear architecture and gene expression modulation [24, 25]. Moreover, a similar structure exists between lncRNAs and mRNAs such as 5' capped, 3' polyadenylated, and multi-exonic [26]. Varying cellular locations of lncRNAs may reflect heterogenous functions and mechanisms in diseases.

Protein ubiquitin plays important roles in different biological processes including cell growth and cycling, embryonic development, tumorigenesis, and protein degradation [27, 28]. UCHL1 has been indicated as a functional ubiquitin balancer and has appeared as a tumor suppressor in HCC, probably via stabilizing p53

Table 3. Expression data of hub genes in HCC tissues and normal controls

Hub gene symbol	HCC tissues			Normal tissues			*P* value
	Mean value	SD	n	Mean value	SD	n	
HRAS	10.0094	0.8335	374	8.7720	0.4761	50	< 0.0001
BMP4	7.9313	1.8434	374	6.7377	1.0537	50	< 0.0001
CALM3	13.1920	0.7412	374	12.5569	0.4510	50	< 0.0001

Note: SD, standard deviation.

[29, 30]. UCHL1 is also beneficial to cell homeostasis of either normal growth or under oxidative stress inner-environments by accumulating p27 [31]. However, as a spliced antisense lncRNA to the UCHL1 gene, no related studies about lncRNA UCHL1-AS1 in HCC have been reported.

In our earlier study, decreased expression of UCHL1-AS1 in HCC cells was proven [10]. In this current study, proliferation and migration of overexpressed UCHL1-AS1 in HCC cells was further detected. We found that high levels of UCHL1-AS1 could effectively inhibit HCC cell mobility. This result implies that lncRNA UCHL1-AS1 might also play a similar inhibitory role in HCC as protein UCHL1. Interestingly, researchers have found antisense lncRNA to UCHL1 in mice could increase UCHL1 synthesis, which means that antisense lncRNAs functioned as a SINEUP, upregulating translation of partially intersected protein-coding mRNAs. Based on these, Aleks Schein et al. first pointed out that natural antisense lncRNAs can also enhance protein translation in human and SINEUPs may exist in a wide variety of mammalian species [32]. Thus, we speculate that lncRNA UCHL1-AS1 may work as a SINEUP to increase UCHL1 expression to further suppress HCC by p53, p27, or other factors.

Meanwhile, genes related to lncRNA UCHL1-AS1 significantly participated in cAMP signaling pathway and Ras signaling pathway. Gene transcription has been principally regulated by cAMP and dysregulated cAMP signaling, closely correlating to hepatic cysto-genesis and steatosis [33-35]. In addition, Ras proteins could adjust proliferation, apoptosis, differentiation, and senescence and aberrant Ras GTPase signal has been well known in tumorigenesis [36, 37]. In HCC, inhibitory effects of V-ATPase could restrain proliferation of tumor cells by hindering membrane related Ras signaling pathways [38].

Compared to normal liver tissues, all hub genes (HRAS, BMP4 and CALM3) were significantly higher in HCC tissues. As a member of Ras oncogene family, HRAS can bind GTP and GDP and they have inherent GTPase activity. GTPases have been identified as intracellular signaling molecules that play crucial roles in regulating cytoskeleton recombination and cell migratory ability [39]. GTPases are widespread in different oncogenes among various cancers and could induce metastasis, invasion, and poor prognosis [40, 41]. Importantly, the overexpressed hub gene BMP4 facilitates HCC cells proliferation, invasion, and metastasis via ID2 [42, 43]. HRAS and BMP4 might be valuable prognosis biomarkers and therapeutic targets for HCC patients. Protein CALM3 regulates cell cycle and cytokinesis, as a key role, and contains multiple alternative splicing transcriptions. All of these evidences hint that hub genes strongly mediate occurrence, progression, and prognosis of HCC. However, the specific molecular mechanisms among 3 hub genes and lncRNA UCHL1-AS1 still require future experimental verification.

Conclusion

Our results suggest that lncRNA UCHL1-AS1 could inhibit HCC cell migration. Moreover, enrichment analysis reveals that HRAS, BMP4, and CALM3 are hub genes of HCC and are closely correlated with HCC.

Acknowledgements

The present study was supported by the National Natural Science Foundation of China (NSFC81560386, NSFC81560489), Natural Science Foundation of Guangxi, China (2017 GXNSFAA198017) and Innovation Project of Graduate Education (YCSW2018103). We also wish to thank public databases such as The Cancer Genome Atlas dataset and the GEPIA.

Disclosure of conflict of interest

None.

Address correspondence to: Drs. Zhenbo Feng and Yiwu Dang, Department of Pathology, The First

Affiliated Hospital of Guangxi Medical University, 6 Shuangyong Road, Nanning 530021, Guangxi Zhuang Autonomous Region, China. Tel: +86 771 5352194; Fax: +86 771 5352194; E-mail: Fengzhenbo_GXMU@163.com (ZBF); dangyiwu@126.com (YWD)

References

[1] Xing M, Kokabi N, Camacho JC and Kim HS. Prospective longitudinal quality of life and survival outcomes in patients with advanced infiltrative hepatocellular carcinoma and portal vein thrombosis treated with Yttrium-90 radioembolization. BMC Cancer 2018; 18: 75.

[2] He B, He Y, Shi W, Gong S, Chen X, Xiao J, Gu J, Ding W and Wang Y. Bioinformatics analysis of gene expression alterations in microRNA122 knockout mice with hepatocellular carcinoma. Mol Med Rep 2017; 15: 3681-3689.

[3] Li JJ, Luo J, Lu JN, Liang XN, Luo YH, Liu YR, Yang J, Ding H, Qin GH, Yang LH, Dang YW, Yang H and Chen G. Relationship between TRAF6 and deterioration of HCC: an immunohistochemical and in vitro study. Cancer Cell Int 2016; 16: 76.

[4] Zhong D and Cen H. Aberrant promoter methylation profiles and association with survival in patients with hepatocellular carcinoma. Onco Targets Ther 2017; 10: 2501-2509.

[5] Dufresne J, Vezina G and Levesque RC. Molecular cloning and expression of the imipenem-hydrolyzing beta-lactamase gene from pseudomonas maltophilia in Escherichia coli. Rev Infect Dis 1988; 10: 806-817.

[6] Lee JS, Heo J, Libbrecht L, Chu IS, Kaposi-Novak P, Calvisi DF, Mikaelyan A, Roberts LR, Demetris AJ, Sun Z, Nevens F, Roskams T and Thorgeirsson SS. A novel prognostic subtype of human hepatocellular carcinoma derived from hepatic progenitor cells. Nat Med 2006; 12: 410-416.

[7] Yang S and Wang XQ. XLF-mediated NHEJ activity in hepatocellular carcinoma therapy resistance. BMC Cancer 2017; 17: 344.

[8] He R, Gao L, Ma J, Peng Z, Zhou S, Yang L, Feng Z, Dang Y and Chen G. The essential role of MTDH in the progression of HCC: a study with immunohistochemistry, TCGA, meta-analysis and in vitro investigation. Am J Transl Res 2017; 9: 1561-1579.

[9] Fang QL, Yin YR, Xie CR, Zhang S, Zhao WX, Pan C, Wang XM and Yin ZY. Mechanistic and biological significance of DNA methyltransferase 1 upregulated by growth factors in human hepatocellular carcinoma. Int J Oncol 2015; 46: 782-790.

[10] Huang Z, Huang L, Wei K, Shen S, Li C, Li W, Li J, Dang Y, Wei Y, Chen G and Feng Z. Downregulation and relationship with clinicopathological parameters of LncRNA UCHL1-AS1 in hepatocellular carcinoma tissues. Int J Clin Exp Pathol 2016; 9: 10290-10297.

[11] Duff MO, Olson S, Wei X, Garrett SC, Osman A, Bolisetty M, Plocik A, Celniker SE and Graveley BR. Genome-wide identification of zero nucleotide recursive splicing in Drosophila. Nature 2015; 521: 376-379.

[12] Fagerberg L, Hallstrom BM, Oksvold P, Kampf C, Djureinovic D, Odeberg J, Habuka M, Tahmasebpoor S, Danielsson A, Edlund K, Asplund A, Sjostedt E, Lundberg E, Szigyarto CA, Skogs M, Takanen JO, Berling H, Tegel H, Mulder J, Nilsson P, Schwenk JM, Lindskog C, Danielsson F, Mardinoglu A, Sivertsson A, von Feilitzen K, Forsberg M, Zwahlen M, Olsson I, Navani S, Huss M, Nielsen J, Ponten F and Uhlen M. Analysis of the human tissue-specific expression by genome-wide integration of transcriptomics and antibody-based proteomics. Mol Cell Proteomics 2014; 13: 397-406.

[13] Li CY, Pang YY, Yang H, Li J, Lu HX, Wang HL, Mo WJ, Huang LS, Feng ZB and Chen G. Identification of miR-101-3p targets and functional features based on bioinformatics, meta-analysis and experimental verification in hepatocellular carcinoma. Am J Transl Res 2017; 9: 2088-2105.

[14] Chen G, Umelo IA, Lv S, Teugels E, Fostier K, Kronenberger P, Dewaele A, Sadones J, Geers C and De Greve J. miR-146a inhibits cell growth, cell migration and induces apoptosis in non-small cell lung cancer cells. PLoS One 2013; 8: e60317.

[15] He R, Yang L, Lin X, Chen X, Lin X, Wei F, Liang X, Luo Y, Wu Y, Gan T, Dang Y and Chen G. MiR-30a-5p suppresses cell growth and enhances apoptosis of hepatocellular carcinoma cells via targeting AEG-1. Int J Clin Exp Pathol 2015; 8: 15632-15641.

[16] Dang Y, Luo D, Rong M and Chen G. Underexpression of miR-34a in hepatocellular carcinoma and its contribution towards enhancement of proliferating inhibitory effects of agents targeting c-MET. PLoS One 2013; 8: e61054.

[17] Huang Z, Huang L, Shen S, Li J, Lu H, Mo W, Dang Y, Luo D, Chen G and Feng Z. Sp1 cooperates with Sp3 to upregulate MALAT1 expression in human hepatocellular carcinoma. Oncol Rep 2015; 34: 2403-2412.

[18] Rueden CT, Schindelin J, Hiner MC, DeZonia BE, Walter AE, Arena ET and Eliceiri KW. ImageJ2: ImageJ for the next generation of scientific image data. BMC Bioinformatics 2017; 18: 529.

[19] Chen J, Sun M, Kent WJ, Huang X, Xie H, Wang W, Zhou G, Shi RZ and Rowley JD. Over 20% of human transcripts might form sense-antisense pairs. Nucleic Acids Res 2004; 32: 4812-4820.

[20] Yelin R, Dahary D, Sorek R, Levanon EY, Goldstein O, Shoshan A, Diber A, Biton S, Tamir Y, Khosravi R, Nemzer S, Pinner E, Walach S, Bernstein J, Savitsky K and Rotman G. Widespread occurrence of antisense transcription in the human genome. Nat Biotechnol 2003; 21: 379-386.

[21] Kumar M and Carmichael GG. Antisense RNA: function and fate of duplex RNA in cells of higher eukaryotes. Microbiol Mol Biol Rev 1998; 62: 1415-1434.

[22] Vanhee-Brossollet C and Vaquero C. Do natural antisense transcripts make sense in eukaryotes? Gene 1998; 211: 1-9.

[23] Latge G, Poulet C, Bours V, Josse C and Jerusalem G. Natural antisense transcripts: molecular mechanisms and implications in breast cancers. Int J Mol Sci 2018; 19.

[24] Chen LL and Carmichael GG. Long noncoding RNAs in mammalian cells: what, where, and why? Wiley Interdiscip Rev RNA 2010; 1: 2-21.

[25] Maenner S, Muller M and Becker PB. Roles of long, non-coding RNA in chromosome-wide transcription regulation: lessons from two dosage compensation systems. Biochimie 2012; 94: 1490-1498.

[26] Guttman M, Amit I, Garber M, French C, Lin MF, Feldser D, Huarte M, Zuk O, Carey BW, Cassady JP, Cabili MN, Jaenisch R, Mikkelsen TS, Jacks T, Hacohen N, Bernstein BE, Kellis M, Regev A, Rinn JL and Lander ES. Chromatin signature reveals over a thousand highly conserved large non-coding RNAs in mammals. Nature 2009; 458: 223-227.

[27] Fang Y and Shen X. Ubiquitin carboxyl-terminal hydrolases: involvement in cancer progression and clinical implications. Cancer Metastasis Rev 2017; 36: 669-682.

[28] Amerik AY and Hochstrasser M. Mechanism and function of deubiquitinating enzymes. Biochim Biophys Acta 2004; 1695: 189-207.

[29] Osaka H, Wang YL, Takada K, Takizawa S, Setsuie R, Li H, Sato Y, Nishikawa K, Sun YJ, Sakurai M, Harada T, Hara Y, Kimura I, Chiba S, Namikawa K, Kiyama H, Noda M, Aoki S and Wada K. Ubiquitin carboxy-terminal hydrolase L1 binds to and stabilizes monoubiquitin in neuron. Hum Mol Genet 2003; 12: 1945-1958.

[30] Yu J, Tao Q, Cheung KF, Jin H, Poon FF, Wang X, Li H, Cheng YY, Rocken C, Ebert MP, Chan AT and Sung JJ. Epigenetic identification of ubiquitin carboxyl-terminal hydrolase L1 as a functional tumor suppressor and biomarker for hepatocellular carcinoma and other digestive tumors. Hepatology 2008; 48: 508-518.

[31] Shen H, Sikorska M, Leblanc J, Walker PR and Liu QY. Oxidative stress regulated expression of ubiquitin carboxyl-terminal Hydrolase-L1: role in cell survival. Apoptosis 2006; 11: 1049-1059.

[32] Schein A, Zucchelli S, Kauppinen S, Gustincich S and Carninci P. Identification of antisense long noncoding RNAs that function as SINEUPs in human cells. Sci Rep 2016; 6: 33605.

[33] Camarena V, Sant DW, Huff TC, Mustafi S, Muir RK, Aron AT, Chang CJ, Renslo AR, Monje PV and Wang G. cAMP signaling regulates DNA hydroxymethylation by augmenting the intracellular labile ferrous iron pool. Elife 2017; 6.

[34] Sun L, Yu CY, Mackey LV and Coy DH. Lanreotide and its potential applications in polycystic kidney and liver diseases. Curr Top Med Chem 2015; 16: 133-140.

[35] Zhang Y, Chen ML, Zhou Y, Yi L, Gao YX, Ran L, Chen SH, Zhang T, Zhou X, Zou D, Wu B, Wu Y, Chang H, Zhu JD, Zhang QY and Mi MT. Resveratrol improves hepatic steatosis by inducing autophagy through the cAMP signaling pathway. Mol Nutr Food Res 2015; 59: 1443-1457.

[36] Schlessinger J. Cell signaling by receptor tyrosine kinases. Cell 2000; 103: 211-225.

[37] Slack C. Ras signaling in aging and metabolic regulation. Nutr Healthy Aging 2017; 4: 195-205.

[38] Bartel K, Winzi M, Ulrich M, Koeberle A, Menche D, Werz O, Muller R, Guck J, Vollmar AM and von Schwarzenberg K. V-ATPase inhibition increases cancer cell stiffness and blocks membrane related Ras signaling-a new option for HCC therapy. Oncotarget 2017; 8: 9476-9487.

[39] Chen R, Wang SJ, Zhang Y, Hou R, Jiang JL and Cui HY. CD147 promotes cell motility via upregulation of p190-B RhoGAP in hepatocellular carcinoma. Cancer Cell Int 2016; 16: 69.

[40] Lu S, Zhou J, Sun Y, Li N, Miao M, Jiao B and Chen H. The noncoding RNA HOXD-AS1 is a critical regulator of the metastasis and apoptosis phenotype in human hepatocellular carcinoma. Mol Cancer 2017; 16: 125.

[41] Shi Y, Qin N, Zhou Q, Chen Y, Huang S, Chen B, Shen G and Jia H. Role of IQGAP3 in metastasis and epithelial-mesenchymal transition in human hepatocellular carcinoma. J Transl Med 2017; 15: 176.

[42] Ma J, Zeng S, Zhang Y, Deng G, Qu Y, Guo C, Yin L, Han Y and Shen H. BMP4 enhances hepatocellular carcinoma proliferation by promoting cell cycle progression via ID2/CDKN1B signaling. Mol Carcinog 2017; 56: 2279-2289.

[43] Zeng S, Zhang Y, Ma J, Deng G, Qu Y, Guo C, Han Y, Yin L, Cai C, Li Y, Wang G, Bonkovsky HL and Shen H. BMP4 promotes metastasis of hepatocellular carcinoma by an induction of epithelial-mesenchymal transition via upregulating ID2. Cancer Lett 2017; 390: 67-76.